Applying Moist Singular Vectors to African Easterly Waves

Rosalind J. Cornforth[1*] and Brian J. Hoskins[2]
[1]*Department of Meteorology, University of Reading, Earley Gate, Reading, Berks. RG6 6BB, UK*
[2]*Grantham Institute for Climate Change, Imperial College, London,, UK*

[*]Correspondence to
Rosalind J. Cornforth,
Department of Meteorology,
University of Reading,
Earley Gate, Reading,
Berks, RG6 6BB, UK.
Tel: +44(0) 118 378 5585.
Fax: +44(0) 118 378 6393.
E-mail:
r.j.Cornforth@reading.ac.uk.

Accepted: 06 June, 2009

Abstract
Moist singular vectors (MSV) have been applied successfully to predicting mid-latitude storms growing in association with latent heat of condensation. Tropical cyclone sensitivity has also been assessed. Extending this approach to more general tropical weather systems here, MSVs are evaluated for understanding and predicting African easterly waves, given the importance of moist processes in their development. First results, without initial moisture perturbations, suggest MSVs may be used advantageously. Perturbations bear similar structural and energy profiles to previous idealised non-linear studies and observations. Strong sensitivities prevail in the metrics and trajectories chosen, and benefits of initial moisture perturbations should be appraised.

Keywords: African easterly waves; singular vectors; moist; AMMA; ECMWF.

1. Introduction

African Easterly waves (AEW) evolve on the African Easterly Jet (AEJ) over tropical North West Africa during the northern hemisphere summer. Their importance lies in their links to the region's convective rainfall, the variability of which can have devastating impacts on the already vulnerable population, and also to tropical cyclogenesis downstream in the north Atlantic. Despite their significance however, weather and climate models continue to have difficulties in simulating the African easterly waves-easterly jet system (AEW-AEJ) and in predicting the basic characteristics of the West African Monsoon (WAM) rainfall due to the wide range of interacting spatio-temporal scales. Recognising the importance of this problem, the international African Multi-disciplinary Monsoon Analysis Project (AMMA) mounted a major observational programme with a Special Observing Period (SOP) in 2006 (Redelsperger et al., 2006). Here we address the imperative of building a strong framework of understanding on which the prediction capabilities of the models may be improved and in which the

observations may be considered. The basic dynamics and physics of the moist AEW-AEJ system is targeted, building on recently gained theoretical insights and exploiting the newly enhanced optimum perturbation moist singular vector technology developed at the European Centre for Medium Range Weather Forecasts (ECMWF).

The current understanding of the interaction of diabatic heating with the AEWs is based on linear and non-linear idealised modelling experiments using normal mode techniques (eg. Cornforth, 2005 and, Cornforth, Hoskins and Thorncroft, 2009, hereafter CHT09). In CHT09, moist waves were shown to grow more rapidly than dry waves and to exhibit deep, vertical structures, there being additional layers of complexity related to the interactions with diabatically-generated PV anomalies. Importantly, the strong interdependence between the AEJ, the AEWs, the moist convection and the upper levels established an *internal variability* on a time-scale of 8-10 days in the model, consistent with a composite analysis (Sultan et al., 2003) showing rainy sequences that lasted, on average, 9 days.

As an alternative to normal mode theory, singular vector perturbations (Farrell, 1982) are investigated that have optimum finite time growth as given by a specified measure. ECMWF developed a singular package that included a linearized version of their physical parametrisations and Puri et al. (2001) successfully exploited it to produce perturbations that, when added to the initial conditions for a forecast, gave an ensemble of tropical cyclone behaviours. Coutinho et al. (2004) considered the impact on extratropical singular vectors of including the parametrised physical processes. It was found that large-scale latent heat release was particularly important and led to enhanced growth and smaller length scales for these moist singular vectors. From here on the singular vectors with parametrised moist processes will be referred to as moist singular vectors (MSVs). It has also been shown (Hoskins and Coutinho, 2005) that, for various high impact European cyclones, MSV perturbations optimised for 24h growth give an insight into their predictability.

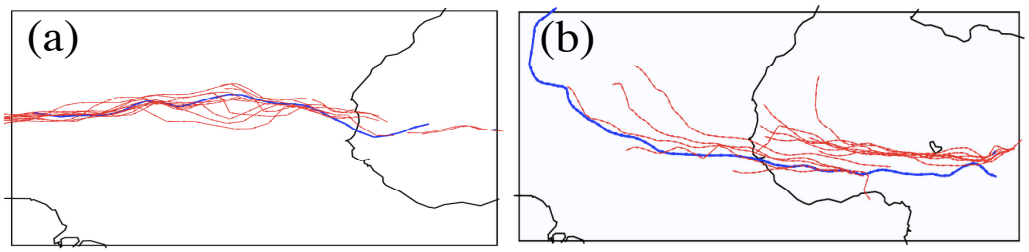

Figure 1: 10-day forecast tracks based on the 700 hPa 2-6 day filtered meridional wind for 2 African easterly waves that evolved in two contrasting (a) dry and (b) wet periods during the 2006 West African monsoon. The 10-day forecasts were made every 12hrs between (a) 9th-15th July 2006 for AEW3; and (b) 1st-10th September for AEW20. Figures courtesy of Kevin Hodges, ESSC, UK who developed the tracking algorithm. The blue lines correspond to the ECMWF analysis, the red lines correspond to the forecasts.

There is now considerable interest in its application for singular vector computation in the tropics and tropical perturbations for the ensemble system on a wider basis than

targeting tropical cyclones. African easterly waves are arguably the tropical systems that exhibit dynamical organization in a manner that is most similar to extra-tropical weather systems, and yet provide the context for convection that is of great importance both in their behaviour, in their impact on society and in yielding ideas on the interaction between physics and dynamics in the tropical atmosphere that may have more general relevance.

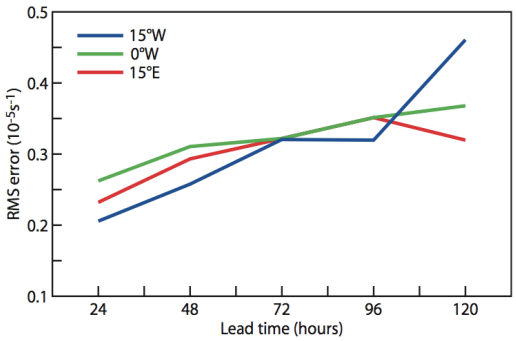

Figure 2: Root mean square errors of 700 hPa curvature vorticity from ECMWF forecast at different ranges with respect to the analysis for three different longitudinal boxes centred on 15°W, the Greenwich Meridian and 15°E. Figure taken from Agustí-Panareda and Beljaars (2008)

The systematic errors that can plague the forecast skill in this region is illustrated by the divergence of the 10-day forecast tracks in Fig. 1. Similarly, in Fig. 2, the root mean square error of the curvature vorticity associated with AEWs exceeds the magnitude of the 700 hPa curvature vorticity of the AEW itself by 48 h in the analysis, rendering the forecast useless (Agusti-Panareda and Beljaars, 2008; Sander and Jones, 2008). The types of errors may be improved by process studies aimed at understanding the fundamental dynamics governing the WAM. Here then, we present first results from a study that aims to use MSVs to build on our theoretical understanding from normal mode studies of the moist AEJ-AEW system, and to learn for practical purposes whether MSVs targeted on W. Africa could be suitable as perturbations to the ECMWF ensemble system for improving AEW prediction and associated rainfall.

2. Approach

The moist singular vectors (MSVs) are calculated using ECMWF's singular package. This is a tangent-linear version of the full, non-linear ECMWF operational forecast tangent linear model (TLM) which newly incorporates full moist physics parameterizations (Mahfouf, 1999) as these give better agreement between the full non-linear forecast model and the TLM. It is important to note that although the initial perturbations are dry, the new moist physics TLM allows the MSV structures to use moisture in their evolution. In these preliminary experiments, the total dry energy (TDE) norm (Buizza and Palmer, 1995) was used at both initial and final times. This choice was made in order to test the validity of the assumption of linearity and address two important questions: (i) whether the TDE metric is relevant for identifying perturbations that are

likely to grow AEWs, and if so, whether it is applicable throughout the monsoon season, or only within dry episodes (eg. early monsoon, or during dry intrusions); and (ii) whether different metrics (eg. TDE, moist norms) would reveal different growth mechanisms operating. These questions have directed the "bottom-up" approach adopted here.

All experiments were run using ECMWF's Cycle 32R3 with 62 levels in the vertical, a time-step of 30 minutes and the horizontal spectral truncation at total wave-number 95 (T95), so that the smallest retained wavelength is about 400 km, which compares with a typical AEW wavelength of 3000 km. The new moist physics package includes linearised parametrizations of vertical diffusion, surface drag, gravity wave drag, large-scale condensation, longwave radiation, and deep cumulus convection. Mahfouf (1999) showed that their inclusion results in a better agreement between the full nonlinear forecast model and the TLM. Optimization times (OTI) for singular vector growth of 24h were applied and the final time amplitudes of the MSVs were constrained by a projection operator (Buizza, 1994a), targeted on the main development region of AEWs (Hopsch et al., 2007), 5-20°N, 20°W-30°E, as marked in Fig. 5(a).

Two AEWs are presented here. These represent the contrasting dry early monsoon (AEW3; Fig. 1(a)) and the fully active moist (AEW20; Fig. 1(b)) monsoon during the AMMA 2006 SOP. These are the basic states for the experiments. It was expected that AEW20 that developed during the moist period would involve more moist and non-linear aspects, and thus provide a suitable test-bed for the TLM with its assumption of linear growth. The two case studies may also be compared with the dry and moist idealized life cycles discussed in CHT09, based on normal mode theory.

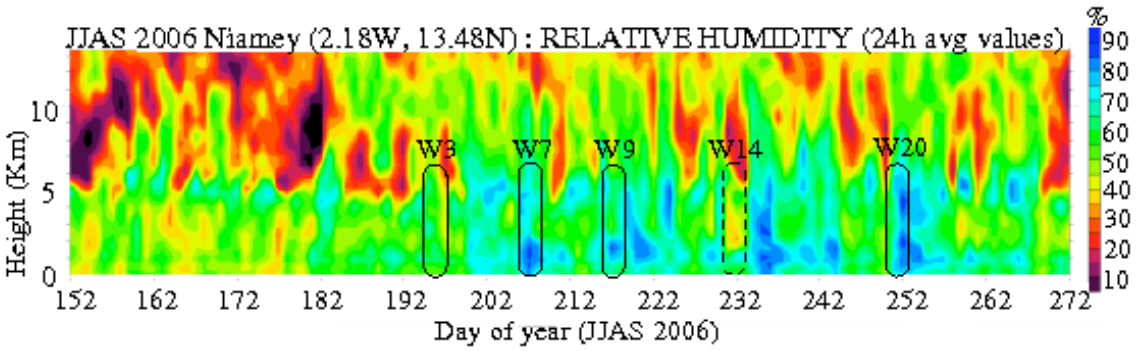

Figure 3: Evolution during JJAS 2006 of the vertical profile of relative humidity at Niamey. Figure kindly provided by Francoise Guichard, IDDRI, France. The black ovals mark the periods of evolution of AEW3 (W3) and AEW20 (W20). The early dry period in which AEW3 evolved contrasts with the later peak monsoon period in which AEW20 evolved. Two further case studies referred to in Fig. 4 are labelled here for completeness (W7, W9). The dotted oval references W14, a future case study.

Their respective evolution periods are marked on Fig. 3, around days 194 (13th July) and 250 (3rd September). Four additional case studies were examined with similar results. Two of these are marked on Fig. 3. These exhibited similar differences and are thus not discussed here, other than through including their amplification factors in Fig. 4.

The earlier period during which AEW3 evolved was predominantly warmer and drier than usual with suppressed convection. The dry mid-troposphere is marked by a thin moist layer around 5 km. From mid-July to mid-September (days 190-158, Fig. 3), the atmosphere became progressively moistened with easterly waves becoming stronger and more coherent from the end of August. AEW20 developed during this time when deep moistening prevailed throughout the lower troposphere, in stark contrast to AEW3. AEW20 originated around 20°E on the 3rd September, reaching the Greenwich Meridian (GM) by the 7th September. It became a tropical depression just south-east of the Cape Verde Islands on the 12th September, before transforming into Tropical Cyclone (TC) Helene. This was the fourth strongest hurricane of the 2006 season, with wind speeds peaking on the 18th September.

The control SV trajectories were initiated for AEW3 and AEW20 when their curvature vorticities exceeded $0.5 \times 10^{-5} s^{-1}$ in the analyses. This follows on from Berry et al. (2007) who found that this value was the best compromise between retaining weaker systems and reducing noise. The structures of the MSV perturbations and their possible mechanisms for growth are discussed in Section 3.

3. Moist Singular Vector Perturbations

The sensitivity of the MSV package to the contrasting basic states is reflected in Fig. 4. This shows the amplification factors associated with the first eight singular vectors (SVs) for the two different case studies. Here, the amplification factor is defined as the ratio between the perturbation norm (the square root of the total dry energy inner product) at the initial time and the perturbation norm at the final time.

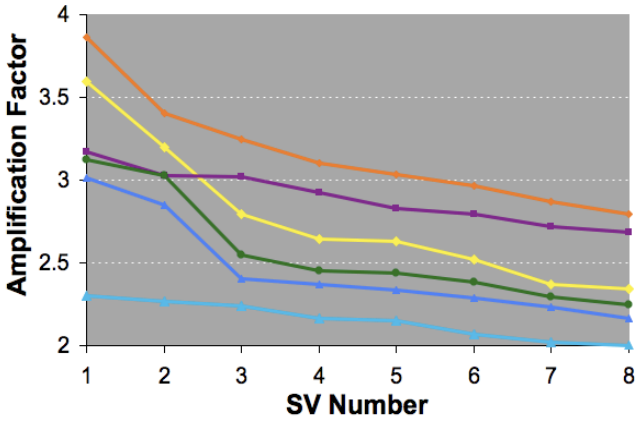

Figure 4: Amplification factors of the first 8 moist singular vectors for AEW3 (20060713, yellow) in the early WAM, and for AEW20 (20060906, turquoise) in the full monsoon. Sensitivity cases with extended target areas (5 to 25N, 35W to 35E) include: AEW3 (20060713, orange), AEW7 (20060728, violet), AEW9 (20060804, green) and AEW20 (20060906, sky blue).

SV amplification factors are generally reduced by approximately a factor of five compared with those for MSVs that develop in baroclinic mid-latitude storms (see Coutinho et al., 2004; and Hoskins and Coutinho, 2005). This may maybe partly associated with the greater stability of the new moist physics SV package used in Cycle 32R3, and partly a result of the different growth mechanisms, particularly in the case of AEW20. The reduced amplification factors for the more non-linear AEWs (AEW7, 9 and 20) suggest that these MSVs are sensitive to something other than the dry energy (TDE) metric used here. This result is consistent with recent results by Ancell and Mass (2008) who found that adjoint sensitivity can vary significantly in structure, magnitude, and location when different, but equally likely, basic-state trajectories are considered.

Results also showed that whilst it was necessary to confine the projection operator to 20°N in the meridional direction to avoid spurious amplification associated with mid-latitude troughs propagating into the region, it was necessary to maintain the longitudinal extent beyond 15°E. This ensures that upstream perturbations triggered by meso-scale convective complexes are included in the MSV optimization region. This was implemented following recent modeling work (Thorncroft et al., 2008) and observational case-studies (Mekonnen et al., 2006) that suggest these upstream perturbations may be as important to AEW genesis, as the mixed barotropic-baroclinic instability mechanisms associated with the AEJ.

In order to learn about the contributions the mixed barotropic-baroclinic conversions made to the MSV growth, the geographical distributions of the total vertically integrated energy for the MSVs for each basic state were compared with distributions of the 24h-averaged baroclinicity and the mean potential vorticity (PV) gradient on the 315 K isentrope (giving indications of the potential for barotropic growth).

In the dry idealized life cycle in CHT09, baroclinic processes dominated the easterly wave growth. In the moist life cycle, the importance of barotropic processes increased in association with a stronger meridional PV gradient through diabatically-generated PV linked to the moist convection in the Intertropical Convergence Zone (ITCZ). In these non-modal experiments, however, the results were unclear. Whilst the MSV perturbations for both AEW3 and AEW20 did indeed grow in regions of higher baroclinicity, they did not propagate downstream towards regions of lower baroclinicity as might be expected, from CHT09 and from mid-latitude analyses (Hoskins et al., 2000). Likewise, according to baroclinic instability theory (Eady, 1949), a doubling in the total energy of a SV in a day might be expected if the MSVs were growing simply as a result of baroclinic processes. Although AEW20's totally vertically integrated energy did double approximately in 24 h. At final time (Fig. 5(e) cf Fig. 5(f)), AEW3 showed a 15-fold increase (Fig. 5(a) cf. Fig. 5(b)) in its total vertically integrated energy. This is far greater than the doubling predicted for baroclinic growth alone (see Badger and Hoskins, 2001; and Eady, 1949). The differential may well be associated with the barotropic processes. The vertically integrated energy distributions were thus compared qualitatively with the basic state Ertel PV for AEW3 and 20 at initial and final times. This confirmed that barotropic processes did have a role to play. The first SVs for both AEW3 and AEW20,

grew in regions of strongly negative meridional PV gradient and moved downstream towards regions of zero PV.

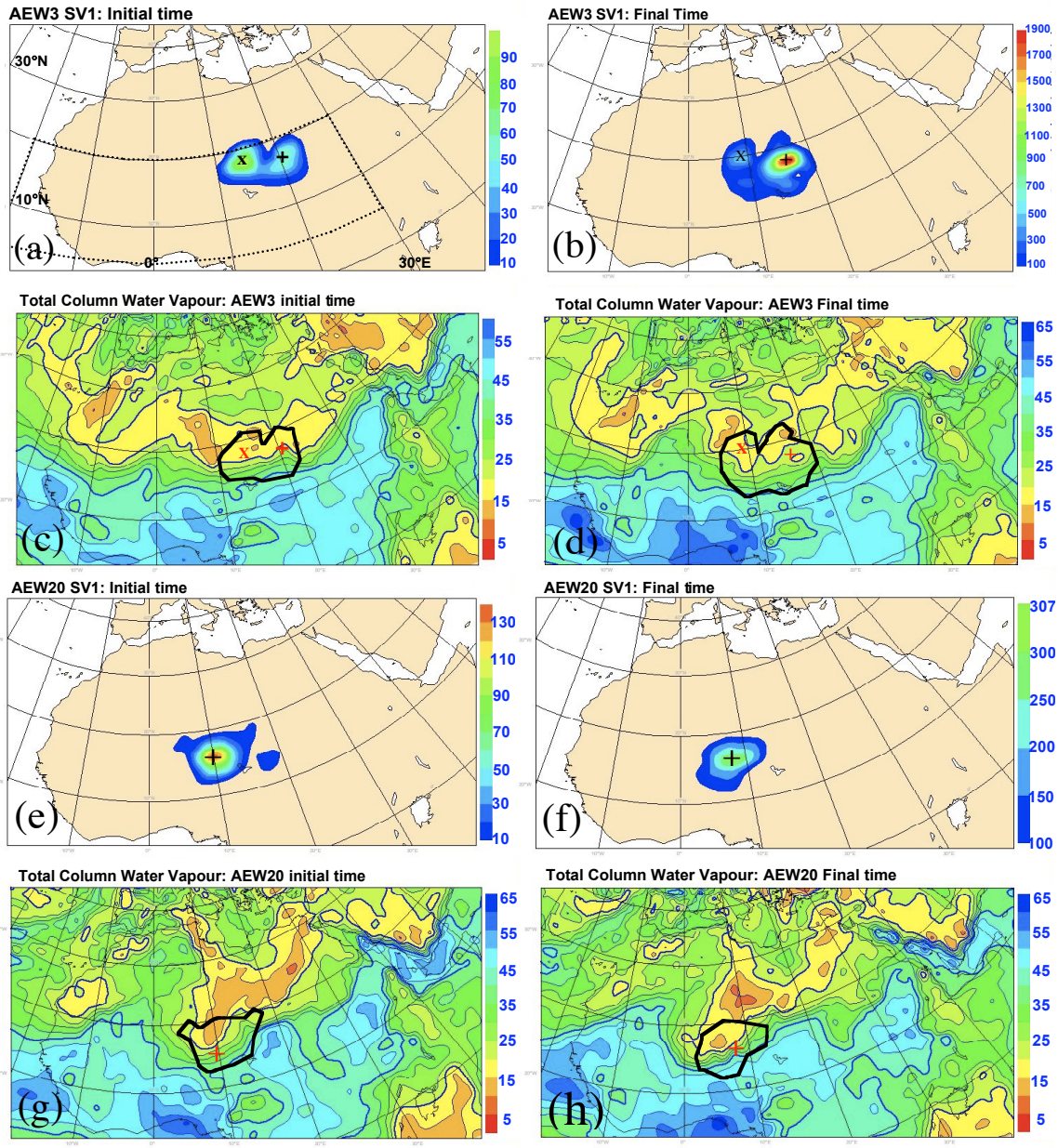

Figure 5: Evidence for some growth mechanisms of the moist singular vector perturbations. The geographical distributions of the vertically integrated energy of the first singular vector for AEW3 and 20 during the early and peak 2006 monsoon periods respectively are shown in (a) at the initial and (b) final times for AEW3. The basic state total column water vapour from the analyses is shown below for the same times in (c) and (d). The fields in panels (a)-(d) are repeated for AEW20 in (e)-(h) respectively. The target area determined by the projection operator is shown as a black dotted line in (a) only.

Since water availability was shown to be important for MSV growth in the mid-latitudes (see Coutinho et al., 2004) and moist AEW's exhibited an internal variability linked to

the growth and decay of rainfall in CHT09, the basic state TCWV at initial and final times was compared with the geographical distributions of the first SVs. These are presented in Figs. 5(a)-(d) for AEW3 and Figs. 5(e)-(h) for AEW20.

SV1 of AEW3 initially has two maxima in its geographical distribution (Fig. 5(a)). The maximum marked '**X**' grows initially in a region of lower water availability and it dissipates at final time (Fig. 5(b)), still in a region of lower water availability (Fig 5(d)). The maximum marked with a cross '**+**' grows initially in a region of higher water availability in comparison (Fig. 5(a)) and persists downstream within this maximum in the local moisture gradient (Fig. 5(d)), such that at final time, SV1 has amplified by an order of magnitude (Fig. 5(b)). For this case study then, the results are consistent with the full physics SV package used and with results in Coutinho et al. (2004); despite the dry initial perturbations, the full physics parameterizations enabled the MSVs to use moisture in the basic state to contribute to its evolution.

The interpretation however, remains difficult for AEW20. Its initial time maximum (Fig. 5(e)) similarly develops within the local moisture gradient but fails to develop explosively as the AEW3 SV1 (compare scale in Fig. 5(f) with Fig. 5(b)). Perhaps this is because the availability of moisture in this region is associated with the cooler temperatures of the low-level south-westerly monsoon flow; a theta-e maximum is associated with a theta minimum. MSV growth is counter-intuitive. It is clear that MSVs are probably more sensitive to something other than total dry energy metric, particularly if AEW-like perturbations are to be captured in the midst of the full monsoon. This will be tested in the next suite of experiments together with a decomposition of the initial MSV structures to extract the quantitative contributions of the different instability mechanisms to the growth of the MSVs.

Horizontal and vertical cross-sections of the MSVs confirmed the contributions of barotropic and baroclinic processes to the SV perturbations growth with typical horizontal and vertical tilts presented against the wind shear (cf. Buizza, 1994a; Buizza and Palmer, 1995). Characteristic baroclinic vertical tilts, weakening by the final time, were observed in the dry perturbations. The moist perturbations were more vertical with increased structural complexity and some amplitude at upper levels around 200 hPa. These results were consistent with the idealized modelling studies in CHT09, and with observations (eg. Reed et al., 1988). In the idealized moist life cycle, the upper levels played an important role in the moist AEW growth in association with diabatically-generated PV.

Despite the difficult interpretaion of growth mechanisms, it is encouraging that the MSV package generated AEW-like perturbations when considered in relation to the analysis. In both the dry and moist basic states, the perturbations strengthened around 0°E. This is consistent with the AEWs main development region (Hopsch et al., 2007). However none of the initial time SV perturbations were located further west despite their presence in the analysis. This is possibly related to the importance of strongly non-linear moist processes causing rapid intensification of the AEWs near the coast which would invalidate the assumption of linear growth for the SVs there. Similar results were found when the moist

basic state was initialized 3 days later when AEW20 was maturing around 7°W and moist convection was very active. The singular vector perturbations generated were extremely weak and dissipated in 24 h.

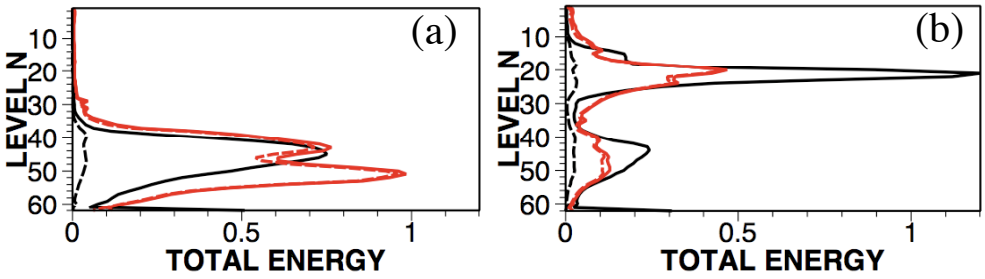

Figure 6: Normalised initial (black) and final (red) time energy profiles as a function of pressure for the first singular vector of (a) AEW 3 and (b) AEW 20. The total energy is shown by solid lines and the kinetic energy component of it by dashed lines.

The vertical distribution of total energy of the first singular vectors for AEW3 and 20 are plotted in Figs. 6(a) and (b) as a function of pressure. These convey the AEW-like nature of the perturbations with maxima at initial time centred near the steering level around Level 44 (750 hPa). This initial energy propagates downwards to Level 51 (900 hPa) as the SV perturbation achieves growth. This is consistent with observations of low-level amplitudes of AEWs (eg. Pytharoulis and Thorncroft, 1999) and modelling studies (eg. Cornforth et al., 2009). In contrast, AEW20 exhibits 2 peaks at initial and final times. These are centred initially around the AEW steering level near 750 hPa, and at upper levels around Level 20 (200 hPa). The mid-troposheric peak is likely to reflect its dAEW-like nature, but unlike the SVs for AEW3, fails to achieve growth as it propagates downwards towards Level 51 (900 hPa, cf. Hartmann et al., 1995). The upper tropospheric peak reflects an idealized mid-latitude MSV analysis by Badger and Hoskins (2001) in which the tropopause peak strengthened as the initial perturbation propagated eastwards and upwards to the tropopause. However, it is likely that this is linked to the outflow of the deep moist convection near the tropopause here. Indeed in CHT09, the vertical extent of the moist waves increased to 200 hPa as they interacted with the diabatically-generated PV. The dissipation of the total energy for AEW20 at final time possibly reflects the need to use a humidity perturbation at initial time for useful SV forecasts during the fully moist monsoon period.

Energy spectra (not shown) plotted as a function of wavenumber for AEW3 show a spectral peak around wavenumber 20 (or a wavelength of 2000 km). This is consistent with the dry linear instability study in CHT09; with observations of AEWs with shorter wavelengths during dry periods (Thorncroft and Hodges, 2001), and with baroclinic growth theory using physically relevant scalings for West Africa (see CHT09). There was a small cascade of energy to larger wavenumbers over the 24h optimization time (OTI) as a result of the physical processes acting in the full moist physics SV package. In contrast, the MSV energy spectra for AEW20 were multi-modal, exhibiting peaks around wavenumbers 12 and 20. This wider range in wavelengths was also found in the idealized moist life cycle in CHT09, associated with greater intermittency in the growth and decay

of moist AEWs linked to the complex relationship between the AEJ, the AEWs, the rainfall and upper tropospheric processes.

In summary, the MSV energy profiles and spectra reflect the AEW-like nature of the perturbations in the dry basic state. In the moist basic state however, the mid- and upper-level peaks were more sensitive to the initial trajectory, projection operator and presence of active convection in the basic state.

Conclusions and Perspectives

In this paper we have presented preliminary results from the application of the ECMWF moist singular vector package to West Africa to address the questions of whether MSVs targeted on W. Africa may be suitable for constructing perturbations to initial conditions for ensemble prediction systems, for understanding and, more generally, for improving forecast skill for the rain-bearing AEWs. This is important to examine given the assumption of linear growth in a region where highly non-linear, moist processes are likely to be important.

In beginning to answer this question, we have analysed the SV perturbations that develop in the early and drier period of the 2006 West African monsoon, and later during its full onset stage. AEW3 developed during the early monsoon when moist convection was suppressed through the intrusion of dry air at mid-levels, and thus represented a relatively dry, more linear regime. AEW20 developed during the peak monsoon in a period of active convection and transformed into TC Helene, the fourth largest hurricane of 2006. This provided a suitable example of a highly non-linear regime. Addressing our question, we examined the optimal choices for the MSV package for application to West Africa and AEWs, the sensitivity of MSVs to the initial basic state, the possible growth mechanisms of the MSV perturbations and therefore what the relevant metrics should be considered.

Perhaps the most basic result is that MSVs can develop AEW-like perturbations and capture the essence of their structure, preferred development region, wavelength and geographical distribution, although there is some dependence on the basic state trajectory and initial set-up parameters. What is not obvious however, is the mechanism for MSV growth. Barotropic, baroclinic and moist processes all contribute just as observed AEWs in which moist convection and latent heat release appear to be important also exhibit both baroclinic and diabatic characteristics (cf. Craig and Cho, 1988; and Snyder and Lindzen, 1991). The difficulty lies in interpreting the MSV growth, given that moisture availability is associated with the cooler temperatures in the low-level southwesterly flow.

Of course, the use of the TDE norm in these experiments should now be reviewed given, for example, the reduction of the amplification factors for AEW20 and the lack of perturbations generated west of 0°E. It can also be argued that the metric or norm chosen should be related to the spatial distribution of expected errors in the analysis.

In the next stage of this study, we are addressing the instability mechanisms in more detail and assessing precipitation changes associated with non-linear integrations. This will help to answer whether the inclusion of MSV perturbations is beneficial to ensemble prediction for forecasts of AEWs and associated rainfall. Future work will include an analysis of TC tracks downstream for cases in which targeted observations include the MSV AEW-like perturbations (Thorncroft and Hodges, 2001).

Acknowledgements

We wish to thank the European Centre for Medium Range Weather Forecasts for the continuing support with the project, and two anonymous referees for their useful comments. We are also grateful for helpful suggestions for future study by George Craig. This work was supported by the Natural Environment Research Council (NERC reference number NE/D010993/1),

References

Agusti-Panareda A, Beljaars A. 2008. ECMWF's Contribution to AMMA. *ECMWF Newsletter No. 115 - Spring 2008* 115: 19-27.

Ancell BC, Mass CF. 2008. The Variability of Adjoint Sensitivity with Respect to Model Physics and Basic-State Trajectory. *Monthly Weather Review* 136: 4612-4628. http://dx.doi.org/10.1175%2F2008MWR2517.1.

Badger J, Hoskins BJ. 2001. Simple Initial Value Problems and Mechanisms for Baroclinic Growth. *Journal of the Atmospheric Sciences* 58: 38-49. http://dx.doi.org/10.1175%2F1520-0469%282001%29058%3C0038%3ASIVPAM%3E2.0.CO%3B2.

Berry G, Thorncroft C, Hewson T. 2007. African Easterly Waves during 2004 - Analysis Using Objective Techniques. *Monthly Weather Review* 135: 1251-1267. http://dx.doi.org/10.1175%2FMWR3343.1.

Buizza R. 1994a. Localization of optimal perturbations using a projection operator. *Quarterly Journal of the Royal Meteorological Society* 120: 1647-1681. http://dx.doi.org/10.1002/qj.49712052010.

Buizza R, Palmer TN. 1995. The Singular-Vector Structure of the Atmospheric Global Circulation. *Journal of the Atmospheric Sciences* 52: 1434-1456. http://dx.doi.org/10.1175%2F1520-0469%281995%29052%3C1434%3ATSVSOT%3E2.0.CO%3B2.

Cornforth RJ. 2005. The African Easterly Jet-African Easterly Wave System. *PhD Thesis* Department of Meteorology, University of Reading.

Cornforth RJ, Hoskins BJ, Thorncroft CD. 2009. The impact of moist processes on the African easterly jet-African easterly wave system. *Quarterly Journal of the Royal Meteorological Society* 135. http://dx.doi.org/10.1002/qj.414.

Coutinho MM, Hoskins BJ, Buizza R. 2004. The Influence of Physical Processes on Extratropical Singular Vectors. *Journal of the Atmospheric Sciences* 61: 195-

209.http://dx.doi.org/10.1175%2F1520-0469%282004%29061%3C0195%3ATIOPPO%3E2.0.CO%3B2.
Craig G, Cho H-R. 1988. Cumulus Heating and CISK in the Extratropical Atmosphere. Part I: Polar Lows and Comma Clouds. *Journal of the Atmospheric Sciences* 45: 2622-2640. http://dx.doi.org/10.1175%2F1520-0469%281988%29045%3C2622%3ACHACIT%3E2.0.CO%3B2.
Eady E. 1949. Long waves and cyclone waves. *Tellus*: 35-52.
Farrell BF. 1982. The Initial Growth of Disturbances in a Baroclinic Flow. *Journal of the Atmospheric Sciences* 39: 1663-1686. http://dx.doi.org/10.1175%2F1520-0469%281982%29039%3C1663%3ATIGODI%3E2.0.CO%3B2.
Hartmann DL, Buizza R, Palmer TN. 1995. Singular Vectors: The Effect of Spatial Scale on Linear Growth of Disturbances. *Journal of the Atmospheric Sciences* 52: 3885-3894. http://dx.doi.org/10.1175%2F1520-0469%281995%29052%3C3885%3ASVTEOS%3E2.0.CO%3B2.
Hopsch SB, Thorncroft CD, Hodges K, Aiyyer A. 2007. West African storm tracks and their relationship to Atlantic tropical cyclones. *Journal of Climate* 20: 2468-2483. <Go to ISI>://WOS:000247159300008.
Hoskins BJ, Coutinho MM. 2005. Moist singular vectors and the predictability of some high impact European cyclones. *Quarterly Journal of the Royal Meteorological Society* 131: 581-601. http://dx.doi.org/10.1256/qj.04.48.
Hoskins BJ, Buizza R, Badger J. 2000. The nature of singular vector growth and structure. *Quarterly Journal of the Royal Meteorological Society* 126: 1565-1580.
Mahfouf J-F. 1999. Influence of physical processes on the tangent-linear approximation. *Tellus A* 51: 147-166. http://dx.doi.org/10.1034/j.1600-0870.1999.00001.x.
Mekonnen A, Thorncroft CD, Aiyyer AR. 2006. Analysis of Convection and Its Association with African Easterly Waves. *Journal of Climate* 19: 5405-5421. http://dx.doi.org/10.1175%2FJCLI3920.1.
Puri K, Barkmeijer J, Palmer TN. 2001. Ensemble prediction of tropical cyclones using targeted diabatic singular vectors. *Quarterly Journal of the Royal Meteorological Society* 127: 709-731. http://dx.doi.org/10.1002/qj.49712757222.
Pytharoulis I, Thorncroft C. 1999. The low-level structure of African easterly waves in 1995. *Monthly Weather Review* 127: 2266-2280.
Redelsperger J-L, Thorncroft CD, Diedhiou A, Lebel T, Parker DJ, Polcher J. 2006. African Monsoon Multidisciplinary Analysis: An International Research Project and Field Campaign. *Bulletin of the American Meteorological Society* 87: 1739-1746. http://dx.doi.org/10.1175%2FBAMS-87-12-1739.
Reed R, Klinker E, Hollingsworth A. 1988. The structure and characteristics of African Easterly Wave disturbances as determined from the ECMWF Operational Analysis/Forecast Syst. *Meteorological Atmosheric Physics* 38: 22-33.
Sander N, Jones SC. 2008. Diagnostic measures for assessing numerical forecasts of African Easterly Waves. *Meteorologische Zeitschrift* 17: 209-220. http://www.ingentaconnect.com/content/schweiz/mz/2008/00000017/00000002/art00011. http://dx.doi.org/10.1127/0941-2948/2008/0269.
Snyder C, Lindzen RS. 1991. Quasi-geostrophic Wave-CISK in an Unbounded Baroclinic Shear. *Journal of the Atmospheric Sciences* 48: 76-86.

http://dx.doi.org/10.1175%2F1520-0469%281991%29048%3C0076%3AQGWCIA%3E2.0.CO%3B2.

Sultan B, Janicot S, Diedhiou A. 2003. The West African Monsoon Dynamics. Part I: Documentation of Intraseasonal Variability. *Journal of Climate* 16: 3389-3406. http://dx.doi.org/10.1175%2F1520-0442%282003%29016%3C3389%3ATWAMDP%3E2.0.CO%3B2.

Thorncroft C, Hodges K. 2001. African Easterly Wave Variability and Its Relationship to Atlantic Tropical Cyclone Activity. *Journal of Climate* 14: 1166-1179. http://dx.doi.org/10.1175%2F1520-0442%282001%29014%3C1166%3AAEWVAI%3E2.0.CO%3B2.

Thorncroft CD, Hall NMJ, Kiladis GN. 2008. Three-Dimensional Structure and Dynamics of African Easterly Waves. Part III: Genesis. *Journal of the Atmospheric Sciences* 65: 3596-3607. http://dx.doi.org/10.1175%2F2008JAS2575.1.